American Mineralogist, Volume 99, pages 16–27, 2014

Minerals in the Human Body

Molecular water in nominally unhydrated carbonated hydroxylapatite: The key to a better understanding of bone mineral†

Jill Dill Pasteris[1,*], Claude H. Yoder[2] and Brigitte Wopenka[1]

[1]Department of Earth and Planetary Sciences, Washington University in St. Louis, St. Louis, Missouri 63130-4899, U.S.A.
[2]Department of Chemistry, Franklin and Marshall College, Lancaster, Pennsylvania 17603, U.S.A.

Abstract

Despite numerous analytical studies, the exact nature of the mineral component of bone is not yet totally defined, even though it is recognized as a type of carbonated hydroxylapatite. The present study addresses the hydration state of bone mineral through Raman spectroscopic and thermogravimetric analysis of 56 samples of carbonated apatite containing from 1 to 17 wt% CO_3, synthesized in H_2O or D_2O. Focus is on the relation between the concentration of molecular water (as distinguished from hydroxyl ions) and the concentration of carbonate in the apatite. Raman spectra confirm the presence of molecular water as part of the crystalline structure in all the aqueously precipitated carbonated apatites. TGA results quantitatively document that, regardless of the concentration of carbonate in the structure, all hydroxylapatites contain ~3 wt% of structurally incorporated water in addition to multiple wt% adsorbed water. We spectroscopically confirmed that natural bone mineral also contains structurally incorporated molecular H_2O based on independent analyses of bone by means of spectral stripping (subtracting the spectrum of collagen from that of bone) and chemical stripping (chemically removing the collagen content of bone prior to analysis). Taken together, the above data support a model in which water molecules densely populate the apatite channels regardless of the abundance of hydroxyl vacancies. We hypothesize that water molecules keep the apatite channels stable even when 80% of the hydroxyl sites are vacant (typical in bone), hinder carbonate ions from substituting for hydroxyl ions in the channels, and help regulate chemical access to the channels (e.g., ion exchange, entry of small molecules). Our results show that bone apatite is not a "flawed hydroxylapatite," but instead a definable mineralogical entity, a combined hydrated-hydroxylated calcium phosphate phase of the form $Ca_{10-x}[(PO_4)_{6-x}(CO_3)_x](OH)_{2-x}\cdot nH_2O$, where n ~ 1.5. Water is therefore not an accidental, but rather an essential, component of bone mineral and other natural and synthetic low-temperature carbonated apatite phases.

Keywords: Apatite, bone, molecular water, channel sites, Raman, thermogravimetric analysis

Introduction

About 55–60 wt% of human bone is mineral, far in excess of the accompanying ~30 wt% collagen and ~10–15 wt% water (Rogers and Zioupos 1999). Its mineral component accounts for much of the load-bearing capacity of bone and also acts as a chemical reservoir of biologically important ions, such as calcium, phosphorus, and magnesium (Skinner 1987; Weiner and Wagner 1998; Rogers and Zioupos 1999; Glimcher 2006). Remarkably, however, there presently still remain analytical and conceptual challenges to understanding both the crystalline structure and composition of bone mineral. The analytical challenges are linked to the extremely small size of the plate-like crystallites of carbonated hydroxylapatite in bone, which are about 2 nm thick and tens of nanometers in the other two directions (Weiner and Wagner 1998; Glimcher 2006; Rey et al. 2009), and their intimate association with an approximately equal volume of the protein collagen. The conceptual challenge comes from the lack of a coherent model of the chemical-structural entity "bone mineral," which is an inorganic compound, yet grows in a biological (aqueous) environment and responds on biological time scales. The history of research in this field during the past 60+ years (Beevers and McIntyre 1946; McConnell 1962; Biltz and Pellegrino 1971; LeGeros et al. 1978; Skinner 1987; Elliott 2002; Cho et al. 2003; Wilson et al. 2006a, 2006b; Glimcher 2006; Rey et al. 2009; Pasteris 2012) reveals an increasing understanding of specific details of the structure and chemistry of bone mineral. Despite all of these analytical studies, however, the exact nature of the mineral component of bone is not yet completely defined.

* E-mail: pasteris@levee.wustl.edu

† Special Collection: Minerals in the Human Body. Special associate editors are Mickey Gunter and Gregory Meeker. Special collection papers can be found on GSW at http://ammin.geoscienceworld.org/site/misc/virtual_special_list.xhtml. Additionally the GSW site has a classification tag found on the right-hand side of the article that is a link to all the collection papers. The MSA website (http://www.minsocam.org/MSA/AmMin/AmMineral.html) has complete information.

0003-004X/14/0001–016$05.00/DOI: http://dx.doi.org/10.2138/am.2014.4627

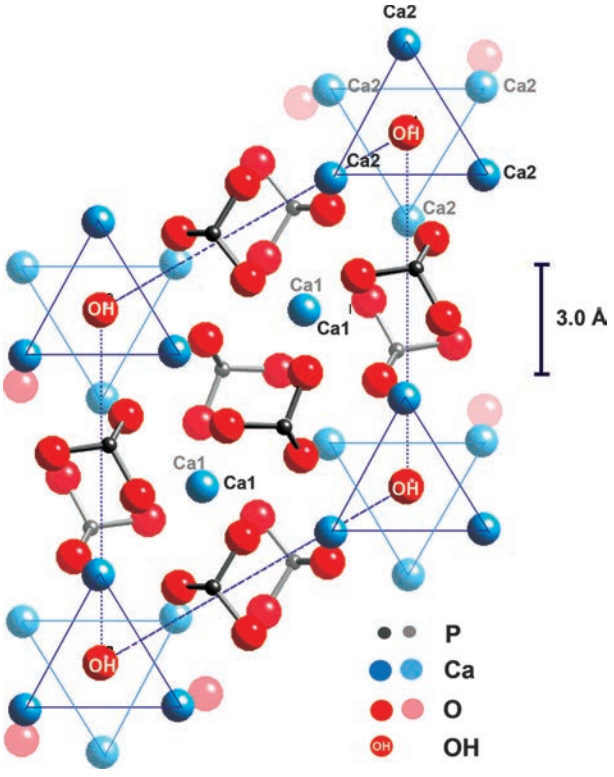

FIGURE 1. Schematic structure of hydroxylapatite (data from Sudarsanan and Young 1969) as viewed down the c-axis. Some calcium ions and portions of phosphate tetrahedra that lie beyond the boundaries (dashed lines) of the unit cell [$(Ca)_{10}(PO_4)_6(OH)_2$] are included here to help define the channels occupied by hydroxyl ions. Six of the calcium ions [referred to as Ca(2) ions] define the channels, and the other four [two in the upper plane and two directly below, referred to as Ca(1) ions] are within the body of the unit cell. Atoms that are closer to the viewer are shaded darker and labeled in black. Each hydroxyl ion resides slightly out of the plane of a triangular array of Ca(2) ions, the two arrays being rotated 60° and displaced from each other by one-half unit along the c-axis. Graphic modified from CrystalMaker for Mac OS X, 6.0.2 (David Palmer, Oxfordshire, U.K.).

It has been known for about a century that bone crystallites are most similar to the mineral hydroxylapatite, $Ca_{10}(PO_4)_6(OH)_2$. Of particular interest in the present study (see Fig. 1) is that there are two different calcium sites in the crystal, labeled Ca(1) and Ca(2), and the hydroxyl ions reside in Ca(2)-defined channels along the c-axis (Skinner 1987; Elliott 2002; Hughes and Rakovan 2002). There are, however, several important differences between hydroxylapatite and biological apatite (Young 1975). Multiple research groups have shown that bone apatite incorporates about 5–8 wt% carbonate (CO_3^{2-}) and that the carbonate dominantly substitutes for phosphate (PO_4^{3-}) tetrahedra in the crystal lattice (LeGeros et al. 1969; Penel et al. 1998; Elliott 2002). It also was realized more than 40 yr ago that bone apatite is deficient in hydroxyl (OH^-) compared to pure hydroxylapatite (Biltz and Pellegrino 1971; Termine and Lundy 1973), but an ongoing controversy ensued concerning exactly how much/little hydroxyl exists in bone mineral and what controls its concentration (Rey et al. 1995, 2009; Pasteris et al. 2004). The most recent evaluations indicate that bone apatite contains only about 20 mol% of the hydroxyl content in stoichiometric hydroxylapatite (Cho et al. 2003). There is therefore about an 80 mol% hydroxyl deficiency in bone apatite. To a large degree, the deficiency in hydroxyl can be explained by the need for charge balance as CO_3^{2-} ions substitute for PO_4^{3-}, which can be represented by the formula $Ca_{10-x}\square_x[(PO_4)_{6-x}(CO_3)_x](OH)_{2-x}\square_x$, where $\square$ represents a vacancy (Rey et al. 1995, 2009; Penel et al. 1998; Elliott 2002; Cazalbou et al. 2004; Pasteris et al. 2012).

There is, however, an additional difference between bioapatite and the anhydrous mineral hydroxylapatite. For over 100 yr, researchers in both the geological and medical fields have argued about whether any of the molecular water (H_2O) that demonstrably is associated with carbonated apatite (both synthetic and in bone) is actually part of its crystallographic structure, rather than just adsorbed on the mineral's surface (McConnell 1952; Biltz and Pellegrino 1971; Joris and Amberg 1971b; LeGeros et al. 1978; Ivanova et al. 2001; Chaikina et al. 2004; Jäger et al. 2006; Wilson et al. 2006a; Zyman et al. 2009; Rey et al. 2009; Pasteris 2012). These decades-old discussions left open the question of whether bone mineral actually contains two different OH species, i.e., hydroxyl ion and molecular water. Interestingly, more than half a century ago the question of whether molecular water existed in low-temperature (biological) apatites also was being investigated with respect to sedimentary carbonated fluorapatite deposits known as phosphorites (McConnell 1952).

The present study approaches the characterization of bone mineral by beginning with analyses of its synthetic equivalents. Subsets of synthetic samples in the present suite were investigated previously to determine the relation between carbonate concentration and hydroxyl concentration in hydroxylapatite (Pasteris et al. 2012) and to identify and quantify structural water in synthetic apatites via nuclear magnetic resonance and thermogravimetric analysis (Yoder et al. 2012a, 2012b). Our primary goals in the current investigation of synthetic carbonated apatite were to investigate in more detail spectroscopically the structural incorporation of water in carbonated hydroxylapatite and fluorapatite, to explore the crystallographic location of water, and to confirm the presence of structural water in actual bone mineral. A major challenge in this work is to discriminate unambiguously between water that is crystallographically incorporated in apatite and water that is adsorbed on the extremely fine-grained synthetic powders. To distinguish between the two, (1) some of the spectroscopic analyses were carried out under dry N_2 gas and (2) some of the apatite samples were synthesized in D_2O solutions. In the latter case, if water did become structurally incorporated, it would have been as D_2O (from the precipitating solution). In contrast, water adsorbed from the air would be H_2O. The ultimate goal of studying synthetic samples is to understand the importance of crystallographically incorporated water in the context of the properties and functionality of bone. Thus, selected data on the synthetic apatite samples were compared with those obtained on actual bone.

EXPERIMENTAL METHODS

Samples

Through aqueous synthesis, we precipitated a suite of carbonated hydroxylapatites and fluorapatites ranging from 1.1 to almost 17 wt% CO_3 (see Table 1) to

TABLE 1. Synthetic carbonated apatite samples

wt% CO_3 from combustion analysis at ±0.2 wt%	Reaction temperature (°C)	Equilibration time (h) in solution
Carbonated hydroxylapatite		
1.1	unknown[a]	unknown[a]
3.0	60	1
3.9[b]	60	2
4.0	60	1
4.0	83	1
4.2	83	1
4.8	85	1
5.0	81	1
6.4	37	2
6.6	63	1
6.9	85	1
8.0	85	1
8.3[b]	60	2
8.5[b]	60	2
9.0[b]	60	2
9.2	82	1
9.6	85	1
10.7	60	2
11	60	1
11.1[b]	60	2
11.4	61	1.25
11.5	60	4
11.6	61	2
11.6	80	2
12	59	3
12.1	61	1
12.8[b]	60	2
13.3	81	2
13.4	60	2
14.0	80	1
14.1	65	2
14.2	63	1
14.8	60	2
15.1	59	2
15.2	60	1
15.3	60	1
15.5	79	2
15.6	60	2
15.6	62	2
16.1	60	2
16.2	65	2
16.2[b]	60	2
16.5	62	2
16.7	60	2
16.9	62	1
18.4	59	2
Carbonated fluorapatite		
1.5	60	2
4.2	60	2
4.7	60	2
7.1[b]	60	2
8.5[b]	60	2
10.4[b]	60	2
10.5	60	2
12.6[b]	60	2
13.6	60	2
16.7	60	2

[a] Preparation methods are not known for this commercial product.
[b] Precipitated from D_2O solution.

determine whether the presence of carbonate in the crystal structure is correlated with the presence of intracrystalline molecular water. For comparison with the synthetic apatites, we analyzed samples of a rat femur and a de-proteinated elk antler (i.e., bone from which the collagen had been chemically removed).

For details of the preparation of carbonated hydroxylapatite, see Yoder et al. (2012b). Briefly, for each desired carbonate to phosphate ratio in the solution, an appropriate weight of $NaHCO_3$ was dissolved in 250 mL of water for the samples precipitated in H_2O. The solution was heated to the desired temperature (either 37, 60, or 85 °C), and its pH was adjusted to 9.0 ± 0.3 with NaOH. To this solution were added 25.0 mL of 0.15 M $Ca(NO_3)_2 \cdot 4H_2O$ and 25.0 mL of 0.09 M $NaH_2PO_4 \cdot H_2O$ (Aldrich, 98%) at a rate of 1 mL/min. For the preparation of carbonated fluorapatite, NaF was used in addition to the above reagents.

For deuterated samples (indicated by a superscript "b" in Table 1), the syntheses were carried out in approximately 10 mL of D_2O heated to the desired temperature, and pH buffering to 9.0 ± 0.5 was accomplished with a 30 wt% solution of NaOD in D_2O. Dehydrated reagents were used where possible, e.g., 10 mL of 0.25 M $Ca(NO_3)_2$ and appropriate mixtures of 0.32 M Na_3PO_4 (or NaH_2PO_4 for fluorapatite) and $NaHCO_3$ of a range of concentrations. For deuterated fluorapatites, a solution of 0.6 M NaF in D_2O was added.

For all samples, when the addition of reagents was complete, the solution was equilibrated at either 37, 60, or 85 ± 3 °C typically for 2 h (see Table 1). The reaction mixture was cooled to room temperature and filtered in a medium porosity glass filter crucible by suction. The product was washed three times with warm water (H_2O or D_2O, as appropriate), air dried in a desiccator for 12 h, and then dried in vacuo at 120 °C for 24 h. Samples then were transferred to screw-cap vials.

Several biological samples were used. The collagen sample (Sigma, C-9879) is type 1, insoluble, from bovine achilles tendon. Cross sections of an elk's antler (shed by a free-ranging animal) and the femur of an adult laboratory rat were analyzed as examples of natural bone mineral. The procedures used for the rat were approved by the animal studies committee of Washington University (Protocol Number: 20100091). An elk's antler was selected for analysis to assure that all the bone material was of the same age, in this case, less than one year because male elks shed their antlers annually. The antler was sawn transversely with a diamond impregnated blade (Buehler Isomet, Lake Bluff, Illinois) to form a wafer 2 cm in diameter and 5 mm thick. For de-proteination ("chemical stripping" of the collagen), the wafer was soaked in 50 mL of 3% H_2O_2 for 18 h, then washed in tap water and air-dried for 24 h. Next it was placed in 50 mL of 5.25% NaClO and run in an ultrasonic cleaner for 1 h, then placed in a fresh aliquot of 50 mL of 5.25% NaClO and soaked for 18 h. Last, it was washed in tap water and air-dried.

Structural and compositional characterization of synthetic samples

A Phillips 3520 X-ray diffractometer (XRD) with monochromator and producing Cu$K\alpha$ radiation (Department of Chemistry, Franklin and Marshall College) was used on each synthetic sample to confirm the identity of the precipitate and to reveal any contaminating phases. Instrumental settings included an analysis range of 2 to 60° 2θ, a step size of 0.02° 2θ, and a dwell time of 1 s. A quartz standard was used to calibrate the diffractometer.

Carbonate analyses of the synthetic apatites were done by Schwarzkopf Microanalytical Laboratories (Woodside, New York) or Galbraith Laboratories (Knoxville, Tennessee) using a C-, H-, N-elemental analyzer on the samples after they had been combusted at 1000 °C in a stream of oxygen. The reported weight percent carbonate concentrations have an experimental uncertainty of 0.2 wt% based on the standard deviation for triplicate analyses of one sample.

For thermogravimetric analyses (TGA), samples were either left in their storage vials or first transferred to another vial before being heated in an oven at 120 °C for 24 h (or dried in vacuo for 48 h). Analysis was done with a TA Instruments Q500 thermogravimetric analyzer (Department of Chemistry, Franklin and Marshall College), calibrated for weight and temperature. Under N_2 gas, samples of 6–8 mg were heated and weighed from room temperature to 1000 °C, typically at a rate of 20 °C/min, but in some instances at 10 °C/min. Weighing measurements have an uncertainty of ±0.4%.

One representative synthetic apatite sample underwent X-ray-fluorescence (XRF) analysis using a Siemens SRS-200 X-ray spectrometer. Details of the sample preparation, data acquisition, and instrument calibration appear in Couture (1993). Briefly, approximately 1 g of powder was ground finer than 200 mesh, dried at 110 °C, and ignited in a ceramic alumina crucible at 925 °C for XRF analysis.

The Raman microprobe used in this study is from Kaiser Optical in Ann Arbor, Michigan (see Pasteris et al. 2012). It consists of a HoloLab Series Research Raman Spectrometer configured for 532 nm laser excitation and covering the spectral range of 0 to 4300 Δcm^{-1} with a resolution of 2.5 cm^{-1}. For this work, we used an Olympus 80× ultra-long-working-distance objective with an N.A. of 0.75 or an Olympus 50× ultra-long-working-distance objective with an N.A. of 0.55. Each Raman analysis represents the average of 32 acquisitions of 4 s each. Every sample underwent 3 to 5 analyses. The laser power was 10 mW at the sample surface, and the beam was focused to about 1 μm by the 80× objective. Most of the Raman analyses were performed under ambient conditions. A selected group of analyses was made after pressed sample powders had resided in a continuous flow of dry nitrogen gas for 2–12 h. Samples were analyzed while the nitrogen gas continued to flow through a glove bag that enclosed the microscope objective, sample, and

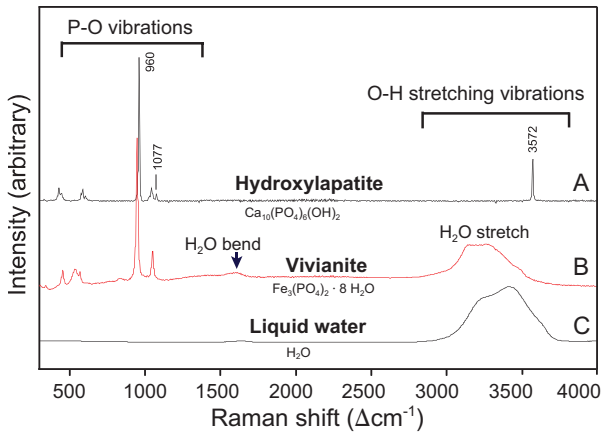

FIGURE 2. Examples of Raman spectra of hydroxylated (**A**) and hydrated phases (**B** and **C**). The presence of phosphate and hydroxyl, respectively, in commercial (Aldrich) hydroxylapatite (**A**) is defined by the occurrence of narrow peaks at ~960 Δcm^{-1} (P-O symmetric stretch for PO_4 tetrahedra in hydroxylapatite) and ~3572 Δcm^{-1} (O-H stretch for hydroxyl ions in the channel sites of hydroxylapatite). Peak widths indicate the degree of atomic ordering within the compound. The narrow O-H stretch peak for hydroxylapatite (**A**) indicates the hydroxyl ion's confinement due to bonding within the crystal, which contrasts with the very broad O-H stretch for liquid water (**C**) and the structural water in some minerals (**B**) in which the molecules are relatively free to move.

laser beam path. The program GRAMS 32 (Galactic, Salem, New Hampshire) was used to deconvolve appropriate Raman peaks into their component spectral bands. The bands were modeled as mixed Gaussian and Lorentzian in form. The spectral envelope of water (e.g., Figs. 2B and 2C) was deconvolved into three bands, which were then summed, whereas the ν_1 P-O stretch was deconvolved into two bands, centered at 950 and 960 Δcm^{-1}, which were summed. These two sums were ratioed to represent the relative concentrations of water associated with the samples.

RESULTS AND DISCUSSION

Characterization

All synthetic samples underwent XRD analysis, which showed them to be poorly crystalline hydroxylapatites without evidence of contaminating phases. One carbonated hydroxylapatite with 6.9 wt% carbonate yielded the following XRF analysis (in wt% values; standard deviation in parentheses, based on triplicate analyses): 2.01(10) Na_2O, 39.87(24) P_2O_5, 50.32(21) CaO, 0.27(15) MgO, 0.03(6) Al_2O_3, 0.12(3) SiO_2, 0.00(0) K_2O, 0.00(0) TiO_2, 0.00(0) Fe_2O_3, 6.15(0) loss on ignition. The Ca/P atomic ratio is 1.60(0.00), whereas that for stoichiometric hydroxylapatite is 1.67.

Further characterization was provided by Raman spectroscopy, which is a well-recognized technique for the analysis and crystallochemical interpretation of apatite, including bone mineral (Nelson and Williamson 1982; Timlin et al. 1999; Carden and Morris 2000; Wopenka and Pasteris 2005; Krajewski et al. 2005; Awonusi et al. 2007). As illustrated in Figure 2A, hydroxylapatite is defined by the occurrence of narrow peaks at ~960 Δcm^{-1} (ν_1 symmetric P-O stretch for PO_4 tetrahedra) and ~3572 Δcm^{-1} (O-H stretch for hydroxyl in the channel site). The Raman spectra in Figure 2 reveal the distinction within the phosphate mineral group between intra-crystalline hydroxyl, as in hydroxylapatite, and intra-crystalline molecular water (showing only weak hydrogen bonding), as in the hydrated phase vivianite. Figure 3 demonstrates that, as carbonate substitutes for PO_4 in apatite, the ν_3 P-O band of hydroxylapatite at ~1077 Δcm^{-1} downshifts to ~1070 Δcm^{-1}. The latter band is believed to represent components of both the phosphate ν_3 and carbonate ν_1 vibrations. The ratio of the area of the 1070 Δcm^{-1} band to that of the 960 Δcm^{-1} P-O band directly correlates with the abundance of carbonate substitution for phosphate in the apatite (Penel et al. 1998; Awonusi et al. 2007). Peak widths broaden as the degree of atomic order (one measure of crystallinity) in the apatite decreases.

Identification/confirmation of crystallographic water

Nominally uncarbonated end-member hydroxylapatite samples purchased from four different commercial manufacturers showed no molecular water in their Raman spectra, i.e., their water concentrations are below the instrument's detection limits, estimated to be approximately 2 wt% in this case. For our aqueously precipitated, carbonated apatite samples, however, the Raman spectrum (see Fig. 3) typically shows an additional broad peak centered at about 3400 Δcm^{-1}, indicative of molecular water. This peak's position and shape are very similar to those of an unconfined drop of water, as illustrated in Figure 2C. The structure of water has been studied for decades via Raman spectroscopy, and the broad peak seen in Figure 2C is known to consist of three separate spectral bands (Walrafen 1964). The detection of the water peak in a spectrum of carbonated apatite depends on multiple factors, including the sample's wt% of carbonate, temperature of precipitation, and drying procedure. Under given synthesis and handling conditions, such as for the sample suite precipitated at 60 °C and shown in Figure 3, an increase in carbonate concentration within the apatite correlates with an increase in its spectroscopically recorded *total* (adsorbed

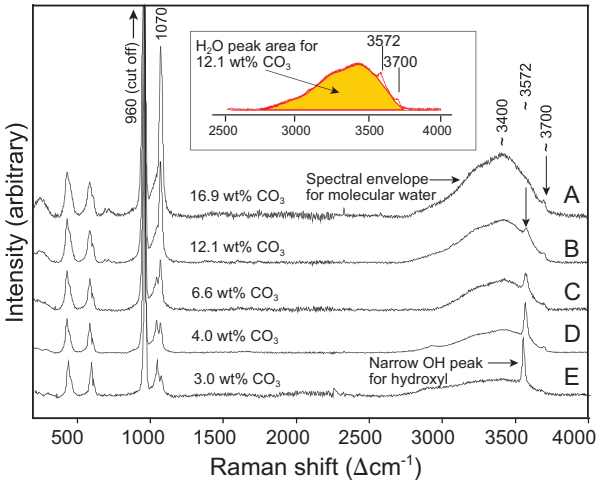

FIGURE 3. Raman spectra of a suite of carbonate-substituted hydroxylapatites, each precipitated at 60 °C. The intensities of all spectra are normalized to the ν_1 P-O stretch vibration at 960 Δcm^{-1}, but spectra are offset along the y-axis for clarity. The intensity of the peak at 1070 Δcm^{-1} indicates the degree of incorporation of carbonate, as substituted for phosphate.

+ crystallographically incorporated) water content.

In addition, as the broad water peak intensifies with increasing carbonate concentration in this apatite suite, a narrow peak develops at about 3700 Δcm^{-1} (Fig. 3). This 3700 Δcm^{-1} peak typically accompanies the 3572 Δcm^{-1} peak that characterizes the O-H stretch of hydroxyl in hydroxylapatite. Over the carbonate compositional range in which they occur together (Figs. 3B–3D), these two narrow peaks consistently have approximately the same shape. As the broad peak for molecular water intensifies, the 3700 Δcm^{-1} peak maintains approximately the same intensity, whereas the 3572 Δcm^{-1} peak gradually weakens until it is no longer detectable (Fig. 3A). The 3700 Δcm^{-1} position does not match that of any hydrated or hydroxylated secondary phase that plausibly might have developed during synthesis of the samples, such as ikaite $CaCO_3 \cdot 6H_2O$ (also not stable at room temperature), monohydrocalcite $CaCO_3 \cdot H_2O$, or portlandite $Ca(OH)_2$ (Coleyshaw et al. 2003; Pasteris et al. 2004). The 3700 Δcm^{-1} peak in the present samples most likely represents H_2O molecules that do not exhibit hydrogen bonding or in which only one of their hydrogen atoms is H-bonded with an anion in the apatite structure, thereby leaving the other OH "dangling" (White 1971; Libowitzky 1999; Perera et al. 2009).

The relative content of total (adsorbed and structurally incorporated) molecular water in the samples was quantified spectroscopically by ratioing the area within the broad envelope of bands representing the O-H stretching vibrations of water (see inset in Fig. 3) against the area for the peak at 960 Δcm^{-1} representing the P-O stretch of phosphate (peak deconvolutions not shown). For the apatites precipitated at 60 °C, an increasing carbonate concentration correlates with increasing amounts of associated molecular water. For a given concentration of incorporated carbonate, the apatite's relative total water content is inversely correlated with the temperature of synthesis. For instance, the synthetic apatite sample that is physiologically the best analog to bone mineral (37 °C precipitation, 6.4 wt% carbonate) reveals remarkably more associated molecular water than the samples precipitated at 60 °C. These correlations with respect to temperature and to carbonate concentration are especially strong for those precipitates equilibrated for only one hour during synthesis.

Our experiments and those of others have shown that an increase in degree of carbonation of apatite typically correlates with decreasing grain size (Baig et al. 1999). Such an increase in the ratio of surface area to volume would encourage adsorption of water. The strong correlation between increasing carbonate substitution in apatite and increasing concentration of total water (Fig. 3) therefore could be due to adsorbed water, structural water, or both. Raman spectroscopic and TGA analyses were applied to distinguish between these possibilities.

We applied two spectroscopic protocols to test which of these water components the observed broad peak (consisting of three spectral bands) centered at ~3400 Δcm^{-1} represents: (1) A subset of the Raman analyses (Fig. 4) of the synthetic powders was carried out first in air ("after synthesis") and then under a continuous flow of dry nitrogen gas ("under N_2"), then after re-equilibration with air again ("in air for 42 h," Fig. 4), and (2) some carbonated apatite samples were synthesized in D_2O and subsequently analyzed. Figure 4 shows the spectral effect of exclusion of atmospheric water vapor from contact with the

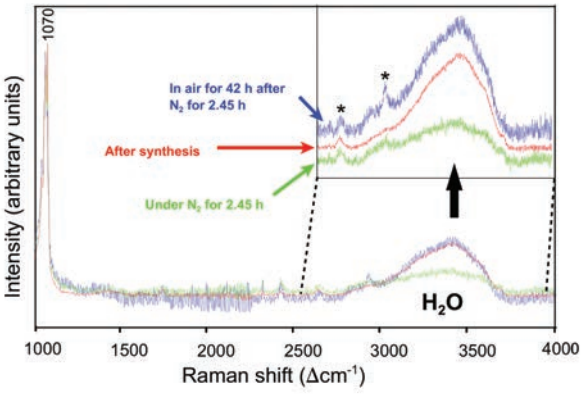

FIGURE 4. Effect of purging a sample of hydroxylapatite (containing 16.1 wt% carbonate) with dry N_2 gas during analysis. Raman spectra of the same carbonated hydroxylapatite sample are compared when it is equilibrated with air (red, blue) and when it is surficially dehydrated by exposure to dry nitrogen gas for 2.45 h (green). All spectra are normalized in intensity with respect to their 1070 Δcm^{-1} peak, permitting direct interspectral comparison of the intensities of the O-H stretch peak for H_2O at ~3400 Δcm^{-1}. Inset shows the normalized spectral traces, but now offset along the y-axis. (* = artifact, such as light intrusion from computer screen and adsorbed hydrocarbons).

apatite, which would eliminate adsorbed water but not affect structural water. All spectra in this figure were obtained on the same aliquot of hydroxylapatite containing 16.1 wt% carbonate. The spectra were normalized to the intensity of the ~1070 Δcm^{-1} peak for incorporated carbonate, so that the intensities of their broad peaks for molecular water at ~3400 Δcm^{-1} can be directly compared. The overlay of three spectra at the bottom of the figure shows that the concentration of water was much lower when the sample was analyzed under dry nitrogen gas (in which it already had undergone active flushing for 2.45 h) than it was after exposure to the ambient air. In the enlarged inset, the individual spectra remain normalized; they simply have been displaced vertically from one another for better visualization. The sample whose adsorbed water had been removed via N_2 purging (bottom spectrum) still contains substantial water, which must be structural. Further tests on the samples showed that the original intensity of the water peak at ~3400 Δcm^{-1} was reproduced after only 5–10 min of re-exposure to the ambient air, i.e., surficial water adsorption on these powders must occur very rapidly. Our confidence in the ability of N_2 purging to remove essentially all adsorbed water is supported by the tests below using deuterium.

The distinction between adsorbed water and structural water also was studied by means of controlling the synthesis process in a suite of fluorapatites. Figure 5 shows Raman spectra from two different highly carbonated fluorapatite samples that were synthesized in D_2O. The broad peak at about 2500 Δcm^{-1} represents the O-D stretch of D_2O, which is down-shifted with respect to the analogous ~3400 Δcm^{-1} position for H_2O. Under these aqueous synthesis conditions, incorporation of "water" into the apatite's crystalline structure during formation means incorporation of D_2O. In contrast, any water adsorbed from the air would be spectroscopically recorded as normal "light" H_2O. In principle, immediately after fluorapatite synthesis and removal from the

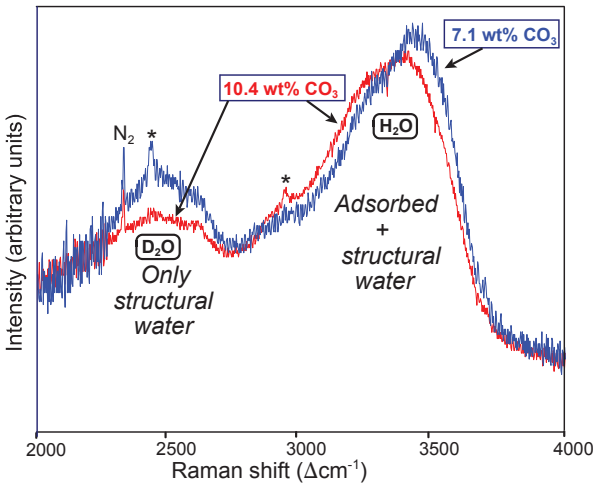

FIGURE 5. Effect of synthesizing the apatite with heavy water. Raman spectra (not normalized) of carbonated fluorapatite samples that were synthesized in D_2O, containing 7.1 and 10.4 wt% carbonate. The spectral positions of the O-D and O-H stretches of D_2O and H_2O, respectively, are shown. Water that was structurally incorporated by the apatite during its crystallization will be dominated by D_2O, but may contain small amounts of (contaminant) H_2O. The adsorbed water, however, will be exclusively in the form of H_2O, as explained in the text. (* = artifact, such as light intrusion from computer screen and adsorbed hydrocarbons).

deuterated aqueous solution, these particles could have adsorbed D_2O on their surfaces. Our experiments, however, indicate that no early adsorbed D_2O was spectroscopically recorded on the apatite powder. This result was verified by our Raman-documented observation of a droplet of D_2O on a glass plate, which showed that H_2O from the air had substituted for all detectable D_2O within minutes. Thus, we concluded that all adsorbed water in the spectra in Figure 5 is in the form of H_2O. The converse, however, cannot be assumed to be true. The typical O-H stretching mode of H_2O at ~3400 Δcm^{-1} is indeed dominated by adsorbed water. There is, however, the possibility that the H_2O peak may also include a minute amount of structurally incorporated water whose light hydrogen was a contaminant in or adsorbent on the carefully dehydrated powdered components used to synthesize the apatite. In summary, all of the D_2O peak and perhaps some very small portion of the H_2O peak record structurally incorporated molecular water in the carbonated apatite.

We previously had established (Yoder et al. 2012a) the structural incorporation of D_2O in several samples of this suite of carbonated fluorapatite and carbonated hydroxylapatite by ^2H solid-state nuclear magnetic resonance (NMR), which detects only the deuterated water component. After such apatite was heated to 500 °C, ^2H NMR detected no deuterium signal (Yoder et al. 2012a), further confirming that the D_2O identified in the unheated sample must be structurally incorporated in the apatite.

Additional information about the molecular environment of the crystallographically incorporated water can be inferred from the relationships of Raman peak positions, shapes, and widths between the two carbonated fluorapatite samples whose spectra are shown in Figure 5. The ~3400 Δcm^{-1} peak in the spectrum of the 10.4 wt% carbonated fluorapatite is downshifted with respect to the comparable peak in the spectrum of the 7.1 wt% carbonated fluorapatite. Analogous relations occur among carbonated hydroxylapatite samples (not shown), ranging from 3.0 to 16.2 wt% CO_3, which have O-H stretching peaks for H_2O that overlap on the high-wavenumber limb, but whose low-wavenumber limbs are increasingly downshifted as carbonate concentration increases. The displacement of the entire O-H stretching peak to lower wavenumbers would indicate strengthening of hydrogen bonding throughout the water component. Note, however, that the base of the right limb of the H_2O peak in Figure 5 remains relatively fixed in position even as the left limb is extended to increasingly lower wavenumbers. Such behavior (shown better in the H_2O than in the D_2O peak) suggests that increasing proportions of the analyzed H_2O molecules are experiencing significant hydrogen bonding. The spectra in Figure 3 furthermore show that, as carbonate concentration increases in the apatite, the hydroxyl (peak at 3572 Δcm^{-1}) concentration decreases. The development of OH-vacancies in the channel sites due to carbonate substitution in the apatite severely alters the crystallographic environment in which the structurally incorporated water molecules are inferred to reside (see Pasteris 2012, Figs. 1 and 2 therein). Increased hydrogen bonding between the incorporated water molecules and the negatively charged O atoms of the phosphate ions in the structure may result from this change within the channel environment, which could account for the downshifts in the H_2O peaks of increasingly carbonated apatites.

Quantification of crystallographically incorporated water

As we have shown recently through thermogravimetric analyses (TGA) on samples in this suite (Yoder et al. 2012b), it is possible to distinguish and quantify water that is adsorbed on apatite and water that is structurally incorporated. In the present study, we have followed the much-used convention in the bioapatite field of regarding water released up to 200 °C as adsorbed and above 200 °C as structurally incorporated (LeGeros et al. 1978). The useful temperature interval in which to measure the release of structural water is terminated by the onset of CO_2 release during carbonate destabilization in the apatite (about 600–650 °C for our samples). For TGA quantification of the amount of structural water in both carbonated hydroxylapatite and fluorapatite, we chose the relatively conservative interval of 200–550 °C, as illustrated by examples in Figure 6. Reported weight losses attributed to structural water have 8 relative % uncertainty based on replicate scans.

Our weight-loss results show that the amounts of adsorbed water are highly variable, as indicated in Figure 6 by the different intersections of the four TGA traces with the 200 °C dashed isotherm. In contrast, the amounts of structural water for these four and indeed all of our carbonated hydroxylapatite samples are essentially constant over a wide range of carbonate concentrations, as illustrated on Figure 6 by the vertical bold red lines delineating the weight loss over 200–550 °C for two samples of very disparate carbonate concentrations. Analogous, but numerically somewhat different, results were obtained on carbonated fluorapatite samples (see Yoder et al. 2012b).

For the purpose of understanding the crystallographic control of molecular water in the apatite structure, the molar proportion of the water is more significant than its weight proportion. Figure

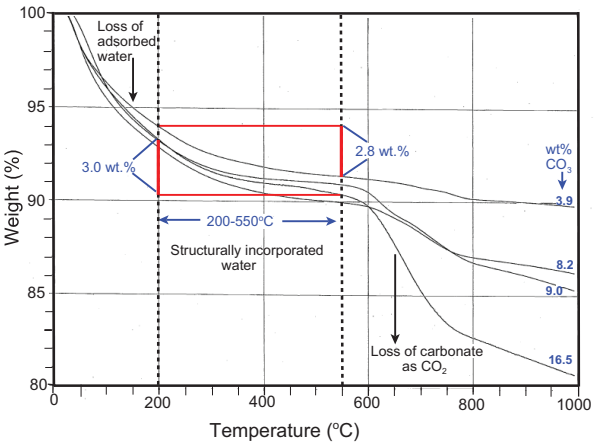

FIGURE 6. Thermogravimetric analyses of carbonated hydroxylapatite samples with 3.9, 8.2, 9.0, and 16.5 wt% carbonate, as labeled on the traces. The water released below 200 °C is regarded as adsorbed and accounts for 6–7 wt% of each sample. Weight loss in the interval 200–550 °C is regarded as structural water. Two selected examples illustrate the weight loss (vertical red line) over the 200–550 °C temperature interval (horizontal red line): 3.0 wt% loss for apatite with 16.5 wt% carbonate and 2.8 wt% loss for apatite with 3.9 wt% carbonate.

7 shows the values in terms of wt% (in blue) and molecular formula units (in red) for structurally incorporated water in carbonated hydroxylapatite (solid symbols) and carbonated fluorapatite samples (open symbols) ranging from about 2 to over 16 wt% carbonate. The structural water in the carbonated hydroxylapatite samples, shown as solid blue circles and approximated by a linear least-squares fit (solid blue line), consistently represents approximately 3 wt% of each sample (variation among samples of 3.08 ± 0.56). As represented by solid red diamonds and approximated by a solid red trend line, this mass is equivalent to about 1.5 molecules of water per unit cell of hydroxylapatite (variation among samples of 1.46 ± 0.29). The latter analysis can be compared to an earlier published model, based on Rietveld structural refinement of neutron diffraction data, in which a carbonated hydroxylapatite sample containing 12.5 wt% carbonate was inferred to contain approximately one molecule of water per unit cell (Wilson et al. 2004). The carbonated fluorapatite responded similarly to the carbonated hydroxylapatite samples for the wt% structural water (open blue circles, dashed blue trend line), i.e., variation among samples of 3.32 ± 0.63 wt%, but the cell occupancy by water (open red diamonds, dashed red trend line) is somewhat higher than in the carbonated hydroxylapatites, i.e., variation among samples of 2.08 ± 0.47 moles per unit cell.

Application to bone mineral

The above results obtained on synthetic hydroxylapatites and fluorapatites of a wide range of carbonate concentrations lead to a better understanding of the nature and amount of molecular water structurally incorporated within apatite that precipitates aqueously under low-temperature conditions. Such findings are of consequence to the properties of natural bone mineral, but only indirectly. The presence of about 25–30 wt% organic components in natural bone complicates testing of the hypothesis that a significant amount of the 10–20 wt% of molecular water in whole bone (Rogers and Zioupos 1999) is actually incorporated within the crystalline structure of the mineral. Published compositional analyses of bone mineral have relied on incineration of the bone to remove (and to measure the masses of) its collagen and water components, leaving "ash" that typically has been regarded as a stand-in for the mineral component, including its composition (Biltz and Pellegrino 1969; Elliott 2002). Such heating usually reaches at least 600 °C and clearly can release (most of the) structural water from the bone mineral, making the residual mineral inappropriate for subsequent analysis of structural water content.

There are also complications in using vibrational spectroscopy to investigate the water concentration in the mineral component in bone. In Raman spectra of bone, the 2800–3800 Δcm^{-1} spectral region, in which the O-H stretch bands of molecular water are located, is dominated by features of the C-H stretches of collagen and the O-H stretches of molecular water contained within the collagen. Not only have those spectral features made it essentially impossible in most cases to detect the O-H stretch of hydroxylapatite at 3572 Δcm^{-1} in Raman or FTIR analyses of bone (Biltz and Pellegrino 1971; LeGeros et al. 1978; Elliott 2002; Pasteris et al. 2004; Rey et al. 2009), but their multiple sources also make it difficult to distinguish which portion of bone's water is incorporated in the mineral itself.

We therefore applied two different approaches to acquiring Raman spectra of isolated bone mineral, i.e., spectral stripping of the peaks arising from collagen and chemical stripping of the collagen itself. Although there are caveats to both of these approaches (e.g., Karampas et al. 2012), it is useful to evaluate their results in the context of the above analyses of synthetic bone-mineral analogs. In spectral stripping, the Raman spectrum of type-1 collagen, which contains its own complement of molecular water (example in Fig. 8B), was subtracted from that of the spectrum of the unprocessed femur bone of a rat (Fig. 8A), so that all organic and water peaks that belong to the collagen were

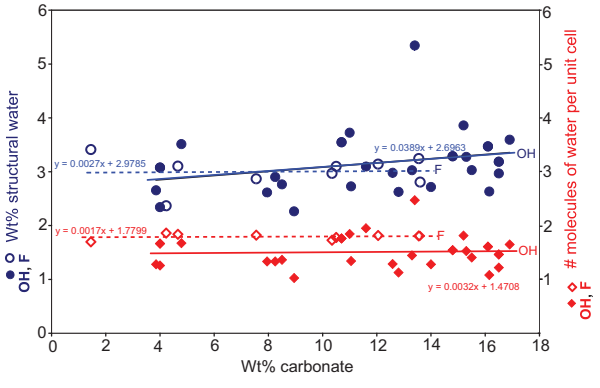

FIGURE 7. Results of TGA measurements on carbonated hydroxylapatite (closed symbols) and carbonated fluorapatite samples (open symbols) precipitated from either H_2O or D_2O solutions. As explained in detail in the text, relations are shown between wt% carbonate in an apatite sample and both its wt% structural water (circles) and its number of moles (n) of water per unit cell of $Ca_{10-x}[(PO_4)_{6-x}(CO_3)_x](OH)_{2-x}\cdot nH_2O$ (diamonds). Linear regressions are shown for each population of points. A subset of these results was published previously in Yoder et al. (2012b).

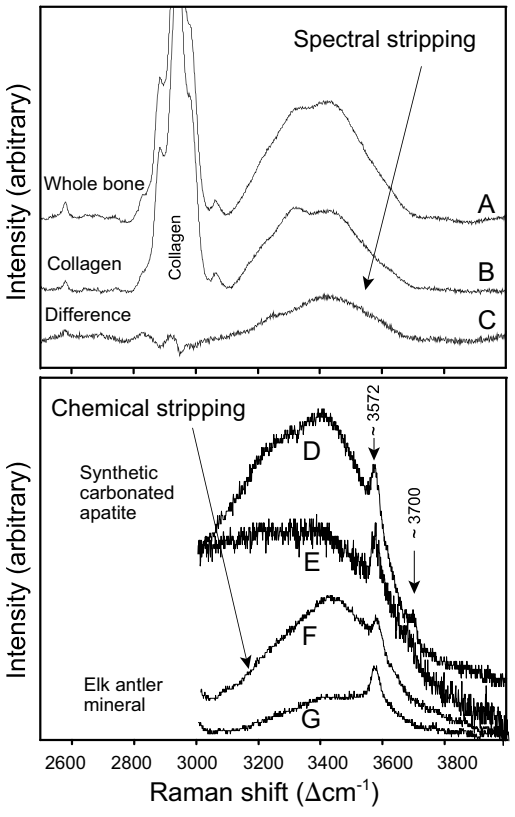

Figure 8. Comparison of the O-H stretch envelope at ~3400 Δcm^{-1} for molecular water in natural bone mineral and synthetic analogs. Spectra are not normalized. The Raman spectra are of (**A**) unprocessed rat femur, (**B**) type-1 collagen, and (**C**) same Raman spectrum as **A** but with the collagen signature totally removed by spectral subtraction, (**D**) synthetic carbonated hydroxylapatite containing 6.4 wt% carbonate that was synthesized at 37 °C and analyzed in air, (**E**) same synthetic apatite but analyzed under dry nitrogen gas after 1 h exposure, (**F**) de-proteinated bone in an elk antler that was analyzed in air, and (**G**) same de-proteinated antler bone but analyzed under dry nitrogen gas after 1 h exposure.

essentially removed. The resultant spectrum (Fig. 8C), which should represent the bone mineral alone, exhibits a significant broad peak in the spectral region of molecular water. The latter no longer can be associated with collagen, but instead must be indicative of water associated with the mineral. The presence of water adsorbed onto the mineral crystallites cannot be ruled out, but it is certainly plausible that some of the water instead resides within the crystalline structure, as documented convincingly in the second spectroscopic approach below.

In chemical stripping (see "Experimental Methods"), the removal of collagen was performed on a transversely sawn cross-sectional slice of bone from the antler of an elk. The Raman spectra of the residual bone material (essentially only mineral) as analyzed in air and subsequently under dry nitrogen gas (after at least 1 h exposure to the flowing gas) are shown in Figures 8F and 8G, respectively. This chemically isolated, but otherwise natural, bone mineral was compared spectroscopically to our best synthetic analog to bone apatite (37 °C precipitate with 6.4 wt% carbonate), also analyzed in air and subsequently under dry nitrogen gas, as shown in Figures 8D and 8E, respectively. Spectra E and G taken on samples after their surficial dehydration by nitrogen gas clearly show a residual component of water centered at ~3400 Δcm^{-1}, which must be structurally incorporated, in both the bone mineral and its synthetic analog.

Development of a new chemical and structural model for bone mineral

There are actually many species of combined hydrated-hydroxylated phosphate minerals, although most of them are quite rare in occurrence. As highlighted by Hawthorne (1998) and Gatta et al. (2013), these phases in both their structure and amount of incorporated water provide important clues to the conditions under which they formed, the point being that modest changes in conditions can destabilize one phosphate phase and cause it to be replaced by another one.

Water as the essential stabilizer in bioapatite

Several crystallographers and NMR spectroscopists (e.g., Joris and Amberg 1971a; Kaflak-Hachulska et al. 2003; Wilson et al. 2006b) have stated that the most likely position for water molecules inside the hydroxylapatite crystal structure is in the channel site in which OH^- ions typically reside (Fig. 1). These channels, approximately 4 Å wide, are large enough for the incorporation of water molecules, as recognized many decades ago (McConnell 1952), given the 1.4 Å radius of both the OH^- ion (Hughes et al. 1989; Hughes and Rakovan 2002) and the water molecule (if hydrogen-bonded, otherwise 1.6 Å; Graziano 2004). Joris and Amberg (1971b) illustrated how the siting of an H_2O molecule could be accommodated within the threefold trigonal planar groups of Ca(2) ions that define each channel of the apatite (see Fig. 1). They also recognized that such placement would encourage H-bonding with the phosphate O atoms of the apatite structure. The spectra of the present study confirm such hydrogen bonding, as discussed for Figure 5.

The next issue was to investigate the mechanism behind water's structural incorporation in apatite. As the degree of carbonate substitution increases in hydroxylapatite, the hydroxyl concentration decreases (Krajewski et al. 2005; Pasteris et al. 2012), which is one of the expected effects due to the need for charge balance. Infrared analyses of bone apatite indicate that only about 15% of the carbonate ions substitute for hydroxyl ions in the channels (Elliott 1994; Rey et al. 2009), and that the dominant substitution mechanism is carbonate for phosphate. In the absence of all but this dominant substitution, every X moles of $(CO_3)^{2-}$ ions that substitute for X moles of $(PO_4)^{3-}$ ions require the generation of X moles of $(OH)^-$ ion vacancies, i.e., $Ca_{10-x}\square_x[(PO_4)_{6-x}(CO_3)_x](OH)_{2-x}\square_x$, where $\square$ represents a vacancy. This relation initially suggested to us that molecular water occupies the vacancies left by hydroxyl ions in the channel sites (a vacancy model also considered by Joris and Amberg 1971b, De Maeyer et al. 1993, and Wilson et al. 2006a), and possibly also the vacancies in Ca(2) sites surrounding the channels. The constancy of the TGA-derived amount of structural water, however, despite the variation in carbonate and hydroxyl concentrations in the apatite (see Fig. 7), rules out the hypothesis that water molecules occupy hydroxyl vacancies. Rather, as discussed in more detail in Yoder et al. (2012b), water molecules appear to

occupy the channels jointly with hydroxyl (or fluoride) ions.

All of our synthetic carbonated hydroxylapatite samples contain approximately 1.5 molecules of H_2O per unit cell (Fig. 7). These observations prompt questions about how water initially enters the apatite structure, why it remains during crystal equilibration, and what (if any) role molecular water plays in the structure or stability of apatite. Such questions require consideration of the process by which carbonated hydroxylapatite forms.

Discussion and debate continue in the biological apatite community concerning whether a precursor phase precedes development of the eventual bone crystallites of carbonated apatite (Weiner 2006; Grynpas 2007). Among those researchers who favor the idea of a precursor phase, some maintain that bioapatite has an amorphous precursor (Termine 1972; Weiner 2006; Olszta et al. 2007; Beniash et al. 2009), whereas others support a crystalline precursor (Brown and Chow 1976; LeGeros et al. 1989; LeGeros 2001; Crane et al. 2006). Note that these two hypotheses are not mutually exclusive; an initially amorphous phase could crystallize into mineral X, which in turn could transform into apatite biologically or under laboratory conditions (Borkiewicz et al. 2010). Intriguingly, water is a key constituent in both the amorphous precursor and crystalline precursor models for the development of bioapatite, as well as other biominerals. With respect to calcium phosphate biomineralization, there is in vitro experimental evidence for an amorphous liquid-like precursor to bone apatite, which later undergoes solidification but does not actually crystallize until (presumably, some of) its water of hydration is expelled (Olszta et al. 2007).

Even in cases in which crystalline precursors to apatite have been hypothesized or, to some extent, documented, they typically are hydrated. Both brushite [$Ca(HPO_4)\cdot 2H_2O$] and octacalcium phosphate [$Ca_8H_2(PO_4)_6\cdot 5H_2O$], i.e., OCP, have been considered as possible precursors to bioapatite over several decades of research (Brown and Chow 1976; Biltz and Pellegrino 1977; Crane et al. 2006; Rey et al. 2009; Borkiewicz et al. 2010; Dorozhkin 2010). Brown and Chow (1976) and Biltz and Pellegrino (1977) made carefully reasoned crystallographic arguments for how OCP could transform into hydroxylapatite. Interestingly, stoichiometric OCP, which contains multiple H_2O molecules of hydration, contains no carbonate. Transformation of OCP into hydroxylapatite might permit incorporation of both carbonate and water into the latter.

Our hypothesis that structural water is important to carbonated apatite is supported by more than the permissive evidence that water becomes incorporated during aqueous precipitation of apatite. A stronger consideration is how the developing apatite crystallites would be affected if water were *not* structurally incorporated. Among the calcium phosphate phases, apatite is distinguished by the presence of channel sites. As questioned many decades ago (Stutman et al. 1962), how can those channels in bone apatite remain stable when populated by only about 15–20% of the hydroxyl ions that do occur in stoichiometric hydroxylapatite (Legros et al. 1987; Cho et al. 2003; Kolmas and Kolodziejski 2007). The channel's integrity is further challenged by the possibly selective vacancy of the channel-surrounding Ca(2) sites as another part of the charge-balance mechanism for phosphate's substitution by carbonate, defined as $Ca_{10-x}\square_x[(PO_4)_{6-x}(CO_3)_x](OH)_{2-x}\square_x$ (see Fig. 1, this article; Figs. 1 and 2 in Pasteris 2012). The fact that water occupies the channels regardless of the amount of carbonate substitution (Fig. 7) therefore could be critical.

The occupancy of the unit cell of carbonated hydroxylapatite by (1.5) H_2O molecules approaches that of OH-ion occupancy (2.0) in stoichiometric hydroxylapatite. This relation suggests two corollaries. First, in hydroxylapatites with very low degrees of carbonation, water molecules essentially must alternate with hydroxyl ions in the channels (Yoder et al. 2012b). Second, in the highly carbonated and atomically disordered form of apatite that constitutes bone mineral, it may be the high population density of H_2O molecules that ultimately stabilizes the OH- and Ca(2)-depleted channels.

The presence of structural water could account for another crystallographically controlled property of bone apatite and carbonated hydroxylapatite synthesized below 100 °C. It may be the physical occupancy of the channels by water that causes CO_3's highly preferential (about 9 to 1) substitution in PO_4 tetrahedra rather than in OH-sites within the channels. Moreover, some studies of the decarbonation reactions of bone and synthetic carbonated apatite during heating indicate that the CO_3 ions initially move from the PO_4 sites to the channels before being released from the apatite as CO_2 (Holcomb and Young 1980; Ivanova et al. 2001; Shi et al. 2005). During heating of carbonated apatite (Fig. 6), the beginning of H_2O release occurs before that of CO_2 (Peters et al. 2000). It is possible that CO_3 ions more readily occupy the channels after H_2O is removed. In the initial organization of ions preliminary to crystallization of apatite at low temperature, the co-incorporation of water may affect the mechanism by which CO_3 is structurally incorporated. With H_2O molecules occupying the channels, the $(PO_4)^{3-}$ sites may become more favorable than channel sites for $(CO_3)^{2-}$ substitution.

There is additional evidence for a mechanistic relation between carbonate and water in bioapatite. Whereas several studies have documented that water concentration in living bone and in its mineral decreases with bone maturity, numerous studies show that carbonate concentration in the mineral increases with maturity (Timmins 1977; Miller et al. 2001; Nyman et al. 2006; Kuhn et al. 2008). There is also evidence that the proportion of carbonate residing in the channel sites (rather than substituting for phosphate) increases with the bone's age (Miller et al. 2001; Kuhn et al. 2008), i.e., as water concentration decreases. Such studies further confirm the inverse correlation between carbonate's and water's occupation of the channels.

Possible underestimation of the amount of water in carbonated apatite

It is well recognized that gradual heating of bone to 1000 °C initially volatilizes the organic components, then evolves CO_2 as carbonate destabilizes in the mineral, and finally produces "ash" with the XRD pattern of end-member highly crystalline hydroxylapatite of considerably larger crystallite size than in the original bone (Rogers and Daniels 2002; Etok et al. 2007; Zyman et al. 2009). Several studies have confirmed not only the high degree of atomic ordering of the final phase, but also that heating causes the hydroxyl concentration in the apatite to increase markedly even as the carbonate concentration decreases (Termine and Lundy 1973; Holcomb and Young 1980; Rey 1994;

Shi et al. 2003; Pasteris et al. 2004; Etok et al. 2007; Kuhn et al. 2008). Quite counterintuitively to the geologist, heating appears to induce hydroxylation rather than de-hydroxylation in the apatite. More importantly for the current discussion, this same phenomenon may contribute to an underestimation of the amount of molecular water that was contained in the original apatite.

The "ash" that remains after the heating of bone to 600–1000 °C is essentially (low-carbonate) hydroxylapatite, but the molar amount of this ash-apatite is less than that of the original bioapatite due to the difference in stoichiometry between the biological and ash apatite phases. The heating of bioapatite with about 6 wt% carbonate substituting only for phosphate and a significant concentration of structurally incorporated water could be represented, according to our model, as

$$2[Ca_9(PO_4)_5(CO_3)(OH)\cdot 1.84H_2O] \rightarrow 1.67[Ca_{10}(PO_4)_6(OH)_2] + 1.3CaO + 2CO_2 + 3H_2O.$$

Thus, 3.68 moles of water in the original 2 moles of carbonated apatite are recorded as only 3 moles of water by combined high-temperature TGA and mass spectroscopy analysis. The remaining 0.68 moles of water were consumed in the rehydroxylation of the apatite. In a typical analysis, those 3 moles of released water are normalized to the original 2 moles of carbonated apatite, yielding 1.5 moles H_2O per unit cell, as we determined in the present study (Fig. 7). The calculation above suggests that there actually were more than 1.5 moles of H_2O in the original, unheated carbonated apatite. The reaction as written also implies that carbonate leaves the apatite, creating a charge imbalance that permits OH^- ions to repopulate the channels, while water is still available in the structure. However, if all the water is released during heating before the carbonate breaks down, as we infer in the TGA study of our synthetic apatites, then the TGA would reflect the true water content.

According to the above reaction, an underestimation of the water content in the original apatite would occur only if water continued to be released above the temperature at which CO_2 was first evolved. The latter situation has been reported in the heating of some synthetic apatites and some actual bone (Holcomb and Young 1980; Mkukuma et al. 2004; Zyman et al. 2009). A proposed alternative mechanism for rehydroxylation of apatite (LeGeros et al. 1978; Kaflak and Kolodziejski 2011), i.e., the reaction of $2(HPO_4)^{2-} + (CO_3)^{2-} \rightarrow (P_2O_7)^{4-} + CO_2 + 2(OH)^-$, would not affect the amount of water detected by TGA.

Implications

Remarkably, we are not the first group to have found evidence for the incorporation of water within crystalline, Ca-deficient apatite, even though no recent review paper on the nature of bone or bone mineral states that structural molecular water is a constituent of bioapatite (e.g., Glimcher 2006; Rey et al. 2009). Mineralogically, early documentation of structurally incorporated water in apatite involved fine-grained, carbonated, and typically fluoride-rich apatites formed in sedimentary phosphorite deposits (McConnell 1952), whose structural water-incorporation recently has been re-confirmed (Mason et al. 2009) and is now supported by our work. Further mineralogical studies on synthetic samples provided insights into the crystallochemical mechanisms that control the amount of molecular water that apatite could contain (Simpson 1968). These studies were both preceded and followed by ones that strongly indicated the structural incorporation of molecular water in bone apatite and in tooth enamel (McConnell 1962; Biltz and Pellegrino 1971; LeGeros et al. 1978). Recent Rietveld analyses have demonstrated that inclusion of water in the unit cell of carbonated apatite will provide a better fit to the crystallographic data (Ivanova et al. 2001; Wilson et al. 2004, 2005, 2006b). With the exception of Ivanova et al. (2001) and Wilson et al. (2006a) for carbonated hydroxylapatite and of Mason et al. (2009) for carbonated fluorapatite, however, there has been little recognition of the possible importance of water's residence in the structure.

The present study and our earlier published work (Yoder et al. 2012b) appear to be the first ones to quantitatively and directly (not by inference) document the concentration of structurally incorporated water in carbonated hydroxylapatites and fluorapatites of a wide range of carbonate compositions. Our work supports the recognition of bone apatite and, more broadly, low-temperature carbonated hydroxylapatite, as a hydrated, hydroxylated phase of approximate composition $Ca_{10-x}[(PO_4)_{6-x}(CO_3)_x](OH)_{2-x}\cdot nH_2O$, similar to what Duncan McConnell (McConnell 1970) proposed 40 yr ago to a clearly non-receptive audience. (His 1970 paper in *American Mineralogist* was entitled "Crystal chemistry of bone mineral: Hydrated carbonate apatites.") The present study suggests that $n \geq 1.5$ over a wide range of carbonate concentrations (3 to >16 wt%). There is reasonable evidence that water is key to stabilizing the vacancy-abundant channels in low-temperature apatite. Water molecules in the channels also apparently favor carbonate substitution for phosphate, while hindering its substitution for hydroxyl, by means of partially excluding carbonate ions from the channels during apatite formation. Structural water appears to occur in a wide compositional (anion and cation) range of apatite-structured compounds, as our ongoing studies confirm.

We propose that the inorganic mineral apatite can respond on biological-biochemical time scales in the vertebrate body in part due to the enhanced ion exchange that is afforded by its comparatively large, water-filled channels. The latter are in direct contact with exchangeable calcium, phosphate, carbonate, and hydroxyl ions in the bioapatite crystal (Fig. 1). It is possible that structurally included water also could aid mineral-organic affinity, especially if any small organic molecules or functional groups of larger molecules could enter the channels (cf. Phillips et al. 2005 concerning calcite). We are presently investigating this possibility. On the other hand, the presence of water molecules in the channels could prevent the entry of other neutral species. In these ways, the inorganic, "non-living" mineral becomes an active, equal participant in the living tissue of bone, able to respond not only through surface exchange but also through water-mediated changes within its structure.

Acknowledgments

The authors acknowledge the Center for Materials Innovation at Washington University and the Lucille and William Hackman Research Fund at Franklin and Marshall College for partial funding of this study. We thank Rex Couture for the XRF analysis, Zhen Li for providing the elk antler spectrum, and Shuyi Liu for help in spectral deconvolution. Special thanks go to Mitchell Sternlieb, Demetra Schermerhorn, Kimberly Worcester, Jennifer Goldenberg, and Zachary Wilt for preparing the experimental samples. The authors thank John Freeman for helpful discussions and John Hughes, associate editor Greg Meeker, and an anonymous reviewer for their comments on an earlier version of the manuscript.

REFERENCES CITED

Awonusi, A., Morris, M.D., and Tecklenburg, M.M.J. (2007) Carbonate assignment and calibration in the Raman spectrum of apatite. Calcified Tissue International, 81, 46–52.

Baig, A.A., Fox, J.L., Young, R.A., Wang, Z., Hsu, J., Higuchi, W.I., Chhettry, A., Zhuang, H., and Otsuka, M. (1999) Relationships among carbonated apatite solubility, crystallite size, and microstrain parameters. Calcified Tissue International, 64, 437–449.

Beevers, C.A., and McIntyre, D.B. (1946) The atomic structure of fluor-apatite and its relation to that of tooth and bone material. Mineralogical Magazine, 27, 254–257.

Beniash, E., Metzler, R.A., Lam, R.S.K., and Gilbert, P. (2009) Transient amorphous calcium phosphate in forming enamel. Journal of Structural Biology, 166, 133–143.

Biltz, R.M., and Pellegrino, E.D. (1969) The chemical anatomy of bone: I. A comparative study of bone composition in sixteen vertebrates. Journal of Bone and Joint Surgery, 51, 456–466.

Biltz, R.M., and Pellegrino, E.D. (1971) The hydroxyl content of calcified tissue mineral. Calcified Tissue International, 36, 259–263.

——— (1977) The nature of bone carbonate. Clinical Orthopaedics, 129, 279–292.

Borkiewicz, O., Rakovan, J., and Cahill, C.L. (2010) Time-resolved in situ studies of apatite formation in aqueous solutions. American Mineralogist, 95, 1224–1236.

Brown, W.E., and Chow, L.C. (1976) Chemical properties of bone mineral. Annual Review of Materials Science, 6, 213–236.

Carden, A., and Morris, M.D. (2000) Application of vibrational spectroscopy to the study of mineralized tissues (review). Journal of Biomedical Optics, 5, 259–268.

Cazalbou, S., Combes, C., Eichert, D., and Rey, C. (2004) Adaptive physico-chemistry of bio-related calcium phosphates. Journal of Materials Chemistry, 14, 2148–2153.

Chaikina, M.V., Khlusov, I.A., Karlov, A.V., and Paichadze, K.S. (2004) Mechanochemical synthesis of nonstoichiometric and substituted apatites with nanosized particles for use as biologically compatible materials. Chemistry for Sustainable Development, 12, 385–394.

Cho, G., Wu, Y., and Ackerman, J.L. (2003) Detection of hydroxyl ions in bone mineral by solid-state NMR spectroscopy. Science, 300, 1123–1127.

Coleyshaw, E., Crump, G., and Griffith, W.P. (2003) Vibrational spectra of the hydrated carbonate minerals ikaite, monohydrocalcite, lansfordite and nesquehonite. Spectrochimica Acta Part A, 59, 2231–2239.

Couture, R.A. (1993) Sample transparency effects in tin determination by X-ray fluorescence. X-ray Spectrometry, 22, 92–96.

Crane, N.J., Popescu, V., Morris, M.D., Steenhuis, P., and Ignelzi, M.A. (2006) Raman spectroscopic evidence for octacalcium phosphate and other transient mineral species deposited during intramembranous mineralization. Bone, 39, 434–442.

De Maeyer, E.A.P., Verbeeck, R.M.H., and Naessens, D.E. (1993) Stoichiometry of Na^+- and CO_3^{2-}-containing apatites obtained by hydrolysis of monetite. Inorganic Chemistry, 32, 5709–5714.

Dorozhkin, S.V. (2010) Amorphous calcium (ortho)phosphates. Acta Biomaterialia, 6, 4457–4475.

Elliott, J.C. (1994) Structure and Chemistry of the Apatites and Other Calcium Orthophosphates, 389 p. Elsevier, New York.

——— (2002) Calcium phosphate biominerals. In M.J. Kohn, J. Rakovan, and J.M. Hughes, Eds., Phosphates—Geochemical, Geobiological, and Materials Importance, 48, p. 427–453. Reviews in Mineralogy and Geochemistry, Mineralogical Society of America, Chantilly, Virginia.

Etok, S.E., Valsami-Jones, E., Wess, T.J., Hiller, J.C., Maxwell, C.A., Rogers, K.D., Manning, D.A.C., White, M.L., Lopez-Capel, E., Collins, M.J., and others. (2007) Structural and chemical changes of thermally treated bone apatite. Journal of Materials Science, 42, 9807–9816.

Gatta, G.D., Nenert, G., and Vignola, P. (2013) Coexisting hydroxyl groups and H_2O molecules in minerals: A single-crystal neutron diffraction study of eosphorite, $MnAlPO_4(OH)_2 \cdot H_2O$. American Mineralogist, 98, 1297–1301.

Glimcher, M.J. (2006) Bone: Nature of the calcium phosphate crystals and cellular, structural, and physical chemical mechanisms in their formation. In N. Sahai and M.A.A. Schoonen, Eds., Medical Mineralogy and Geochemistry, 64, p. 223–282. Reviews in Mineralogy and Geochemistry, Mineralogical Society of America, Chantilly, Virginia.

Graziano, G. (2004) Water: Cavity size distribution and hydrogen bonds. Chemical Physics Letters, 396, 226–231.

Grynpas, M. (2007) Transient precursor strategy or very small biological apatite crystals? Bone, 41, 162–164.

Hawthorne, F.C. (1998) Structure and chemistry of phosphate minerals. Mineralogical Magazine, 62, 141–164.

Holcomb, D.W., and Young, R.A. (1980) Thermal decomposition of human tooth enamel. Calcified Tissue International, 31, 189–201.

Hughes, J.M., and Rakovan, J. (2002) The crystal structure of apatite, $Ca_5(PO_4)_3(F,OH,Cl)$. In M.J. Kohn, J. Rakovan, and J.M. Hughes, Eds., Phosphates—Geochemical, Geobiological, and Materials Importance, 48, p. 1–12. Reviews in Mineralogy and Geochemistry, Mineralogical Society of America, Chantilly, Virginia.

Hughes, J.M., Cameron, M., and Crowley, K.D. (1989) Structural variations in natural F, OH, and Cl apatites. American Mineralogist, 74, 870–876.

Ivanova, T.I., Frank-Kamenetskaya, O.V., Kol'tsov, A.B., and Ugolkov, V.L. (2001) Crystal structure of calcium-deficient carbonated hydroxyapatite. Thermal decomposition. Journal of Solid State Chemistry, 160, 340–349.

Jäger, C., Welzel, T., Meyer-Zaika, W., and Epple, M. (2006) A solid-state NMR investigation of the structure of nanocrystalline hydroxyapatite. Magnetic Resonance in Chemistry, 44, 573–580.

Joris, S.J., and Amberg, C.H. (1971a) The nature of deficiency in non-stoichiometric hydroxyapatites. I. Catalytic activity of calcium and strontium hydroxyapatites. Journal of Physical Chemistry, 75, 3167–3171.

——— (1971b) The nature of deficiency in nonstoichiometric hydroxyapatites. II. Spectroscopic studies of calcium and strontium hydroxyapatites. Journal of Physical Chemistry, 75, 3172–3178.

Kaflak, A., and Kolodziejski, W. (2011) Complementary information on water and hydroxyl groups in nanocrystalline carbonated hydroxyapatites from TGA, NMR and IR measurements. Journal of Molecular Structure, 990, 263–270.

Kaflak-Hachulska, A., Samoson, A., and Kolodziejski, W. (2003) ^1H MAS and ^1H to ^{31}P CP/MAS NMR study of human bone mineral. Calcified Tissue International, 73, 476–486.

Karampas, I.A., Orkoula, M.G., and Kontoyannis, C.G. (2012) Effect of hydrazine based deproteination protocol on bone mineral crystal structure. Journal of Materials Science: Materials in Medicine, 23, 1139–1148.

Kolmas, J., and Kolodziejski, W. (2007) Concentration of hydroxyl groups in dental apatites: A solid-state ^1H MAS NMR study using inverse $^{31}P-{}^1H$ cross-polarization. Chemical Communications, 2007, 4390–4392.

Krajewski, A., Mazzocchi, M., Buldini, P.L., Ravaglioli, A., Tinti, A., Taddei, P., and Fagnano, C. (2005) Synthesis of carbonated hydroxyapatites: Efficiency of the substitution and critical evaluation of analytical methods. Journal of Molecular Structure, 744-747, 221–228.

Kuhn, L., Grynpas, M.D., Rey, C.C., Wu, Y., Ackerman, J.L., and Glimcher, M.J. (2008) A comparison of the physical and chemical differences between cancellous and cortical bovine bone mineral at two ages. Calcified Tissue International, 83, 146–154.

LeGeros, R.Z. (2001) Formation and transformation of calcium phosphates: Relevance to vascular calcification. Zeitschrift für Kardiologie, Suppl. 2, III116-III124.

LeGeros, R.Z., Trautz, O.R., Klein, E., and LeGeros, J.P. (1969) Two types of carbonate substitution in the apatite structure. Experientia, 25, 5–7.

LeGeros, R.Z., Bonel, G., and Legros, R. (1978) Types of "H_2O" in human enamel and in precipitated apatites. Calcified Tissue International, 26, 111–118.

LeGeros, R.Z., Daculsi, G., Orly, I., Abergas, T., and Torres, W. (1989) Solution-mediated transformation of octacalcium phosphate (OCP) to apatite. Scanning Electron Microscopy, 3, 129–138.

Legros, R., Balmain, N., and Bonel, G. (1987) Age-related changes in mineral of rat and bovine cortical bone. Calcified Tissue International, 41, 137–144.

Libowitzky, E. (1999) Correlation of O-H stretching frequencies and O-H···O hydrogen bond lengths in minerals. Monatshefte für Chemie, 130, 1047–1059.

Mason, H.E., McCubbin, F.M., Smirnov, A., and Phillips, B.L. (2009) Solid-state NMR and IR spectroscopic investigation of the role of structural water and F in carbonate-rich fluorapatite. American Mineralogist, 94, 507–516.

McConnell, D. (1952) The problem of the carbonate apatites. IV. Structural substitutions involving CO_2 and OH. Bulletin de la Societe Francaise de Mineralogie et Cristallographie, 7-9, 428–445.

——— (1962) The crystal structure of bone. Clinical Orthopaedics, 23, 253–268.

——— (1970) Crystal chemistry of bone mineral: Hydrated carbonate apatites. American Mineralogist, 55, 1659–1669.

Miller, L.M., Vairavamurthy, V., Chance, M.R., Mendelsohn, R., Paschelis, E.P., Betts, F., and Boskey, A. (2001) In situ analysis of mineral content and crystallinity in bone using infrared micro-spectroscopy of the ν_4 PO_4^{3-} vibration. Biochimica et Biophysica Acta, 1527, 11–19.

Mkukuma, L.D., Skakle, J.M.S., Gibson, I.R., Imrie, C.T., Aspden, R.M., and Hukins, D.W.L. (2004) Effect of the proportion of organic material in bone on thermal decomposition of bone mineral: An investigation of various bones from different species using thermogravimetric analysis coupled to mass spectrometry, high-temperature X-ray diffraction, and Fourier transform infrared spectroscopy. Calcified Tissue International, 75, 321–328.

Nelson, D.G.A., and Williamson, B.E. (1982) Low-temperature laser Raman spectroscopy of synthetic carbonated apatites and dental enamel. Australian Journal of Chemistry, 35, 715–727.

Nyman, J.S., Roy, A., Shen, X., Acuna, R.L., Tyler, J.H., and Wang, X. (2006) The influence of water removal on the strength and toughness of cortical bone. Journal of Biomechanics, 39, 931–938.

Olszta, M.J., Cheng, X., Jee, S.S., Kumar, R., Kim, Y.-Y., Kaufman, M.J., Douglas, E.P., and Gower, L.B. (2007) Bone structure and formation: A new perspective. Materials Science and Engineering: R: Reports, 58, 77–116.

Pasteris, J.D. (2012) Structurally incorporated water in bone apatite: A cautionary tale. In R.B. Heimann, Ed., Calcium Phosphates: Structure, Synthesis, Properties, and Applications, p. 63–94, Nova Science, New York.
Pasteris, J.D., Wopenka, B., Freeman, J.J., Rogers, K., Valsami-Jones, E., van der Houwen, J.A.M., and Silva, M.J. (2004) Lack of OH in nanocrystalline apatite as a function of degree of atomic order: Implications for bone and biomaterials. Biomaterials, 25, 229–238.
Pasteris, J.D., Yoder, C.H., Sternlieb, M.P., and Liu, S. (2012) Effect of carbonate incorporation on the hydroxyl content of hydroxylapatite. Mineralogical Magazine, 76, 2741–2759.
Penel, G., Leroy, G., Rey, C., and Bres, E. (1998) MicroRaman spectral study of the PO_4 and CO_3 vibrational modes in synthetic and biological apatites. Calcified Tissue International, 63, 475–481.
Perera, P.N., Fega, K.R., Lawrence, C., Sundstrom, E.J., Tomlinson-Phillips, J., and Ben-Amotz, D. (2009) Observation of water dangling OH bonds around dissolved nonpolar groups. Proceedings of the National Academy of Sciences, 106, 12230–12234.
Peters, F., Schwarz, K., and Epple, M. (2000) The structure of bone studied with synchrotron X-ray diffraction, X-ray absorption spectroscopy and thermal analysis. Thermochimica Acta, 361, 131–138.
Phillips, B.L., Lee, Y.J., and Reeder, R.J. (2005) Organic coprecipitates with calcite: NMR spectroscopic evidence. Environmental Science & Technology, 39, 4533–4539.
Rey, C. (1994) Apatite channels and zeolite-like properties. In P.W. Brown and B. Constanz, Eds., Hydroxyapatite and Related Materials, p. 257–262, CRC Press, Boca Raton, Florida.
Rey, C., Miquel, J.L., Facchini, L., Legrand, A.P., and Glimcher, M.J. (1995) Hydroxyl groups in bone mineral. Bone, 16, 583–586.
Rey, C., Combes, C., Drouet, C., and Glimcher, M.J. (2009) Bone mineral: Update on chemical composition and structure. Osteoporosis International, 20, 1013–1021.
Rogers, K.D., and Daniels, P. (2002) An X-ray diffraction study of the effects of heat treatment on bone mineral microstructure. Biomaterials, 23, 2577–2585.
Rogers, K., and Zioupos, P. (1999) The bone tissue of the rostrum of a *Mesoplodon densirostris* whale: A mammalian biomineral demonstrating extreme texture. Journal of Materials Science Letters, 18, 651–654.
Shi, J., Klocke, A., Zhang, M., and Bismayer, U. (2003) Thermal behavior of dental enamel and geologic apatite: An infrared spectroscopic study. American Mineralogist, 88, 1866–1871.
——— (2005) Thermally-induced structural modification of dental enamel apatite: Decomposition and transformation of carbonate groups. European Journal of Mineralogy, 17, 769–775.
Simpson, D.R. (1968) Substitutions in apatite: I. Potassium-bearing apatite. American Mineralogist, 53, 432–444.
Skinner, H.C.W. (1987) Bone: Mineralization. In J.A. Albright and R.A. Brand, Eds., The Scientific Basics of Orthopaedics, p. 199–211. Appleton and Lange Press, Norwalk, Connecticut.
Stutman, J.M., Posner, A.S., and Lippincott, E.R. (1962) Hydrogen bonding in the calcium phosphates. Nature, 193, 368–369.
Sudarsanan, K., and Young, R.A. (1969) Significant precision in crystal structural details: Holly Springs hydroxyapatite. Acta Crystallographica, B25, 1534–1543.
Termine, J.D. (1972) Mineral chemistry and skeletal biology. Clinical Orthopaedics and Related Research, 85, 207–239.
Termine, J.D., and Lundy, D.R. (1973) Hydroxide and carbonate in rat bone mineral and its synthetic analogues. Calcified Tissue International, 13, 73–82.
Timlin, J.A., Carden, A., and Morris, M.D. (1999) Chemical microstructure of cortical bone probed by Raman transects. Applied Spectroscopy, 53, 1429–1435.
Timmins, P.A. (1977) Bone water. Calcified Tissue International, 23, 1–5.
Walrafen, G.E. (1964) Raman spectral studies of water structure. Journal of Chemical Physics, 40, 3249–3256.
Weiner, S. (2006) Transient precursor strategy in mineral formation of bone. Bone, 39, 431–433.
Weiner, S., and Wagner, H.D. (1998) The material bone: Structure-mechanical function relations. Annual Review of Materials Science, 28, 271–298.
White, W.B. (1971) Infrared characterization of water and hydroxyl ion in the basic magnesium carbonate minerals. American Mineralogist, 56, 46–53.
Wilson, R.M., Elliott, J.C., Dowker, S.E.P., and Smith, R.I. (2004) Rietveld structure refinement of precipitated carbonate apatite using neutron diffraction data. Biomaterials, 25, 2205–2213.
Wilson, R.M., Elliott, J.C., Dowker, S.E.P., and Rodriguez-Lorenzo, L.M. (2005) Rietveld refinements and spectroscopic studies of the structure of Ca-deficient apatite. Biomaterials, 26, 1317–1327.
Wilson, E.E., Awonusi, A., Morris, M.D., Kohn, D.H., and Tecklenburg, M.M.J. (2006a) Three structural roles for water in bone observed by solid-state NMR. Biophysical Journal, 90, 3722–3731.
Wilson, R.M., Dowker, S.E.P., and Elliott, J.C. (2006b) Rietveld refinements and spectroscopic structural studies of a Na-free carbonate apatite made by hydrolysis of monetite. Biomaterials, 27, 4682–4692.
Wopenka, B., and Pasteris, J.D. (2005) A mineralogical perspective on the apatite in bone. Materials Science and Engineering C, 25, 131–143.
Yoder, C.H., Pasteris, J.D., Worcester, K.N., and Schermerhorn, D.V. (2012a) Structural water in carbonated hydroxylapatite and fluorapatite: Confirmation by solid state ^{2}H NMR. Calcified Tissue International, 90, 60–67.
Yoder, C.H., Pasteris, J.D., Worcester, K.N., Schermerhorn, D.V., Sternlieb, M.P., Goldenberg, J.E., and Wilt, Z.T. (2012b) Dehydration and rehydration of carbonate fluor- and hydroxylapatite. Minerals, 2, 100–117.
Young, R.A. (1975) Biological apatite vs. hydroxyapatite at the atomic level. Clinical Orthopaedics and Related Research, 113, 249–262.
Zyman, Z.Z., Rokhmistrov, D.V., Glushko, V.I., and Ivanov, I.G. (2009) Thermal impurity reactions and structural changes in slightly carbonated hydroxyapatite. Journal of Materials Science: Materials in Medicine, 20, 1389–1399.

Manuscript received June 5, 2013
Manuscript accepted August 24, 2013
Manuscript handled by Gregory Meeker